Magnetic superelasticity and inverse magnetocaloric effect in Ni-Mn-In

Thorsten Krenke, Eyüp Duman, Mehmet Acet, and Eberhard F. Wassermann
Experimentalphysik, Universität Duisburg-Essen, D-47048 Duisburg, Germany

Xavier Moya, Lluís Mañosa, and Antoni Planes
Facultat de Física, Departament d'Estructura i Constituents de la Matèria, Universitat de Barcelona, Diagonal 647, E-08028 Barcelona, Catalonia, Spain

Emmanuelle Suard and Bachir Ouladdiaf
Institut Laue-Langevin, BP 156, 38042 Grenoble Cedex 9, France

(Received 22 March 2006; revised manuscript received 2 December 2006; published 20 March 2007)

Applying a magnetic field to a ferromagnetic $Ni_{50}Mn_{34}In_{16}$ alloy in the martensitic state induces a structural phase transition to the austenitic state. This is accompanied by a strain which recovers on removing the magnetic field, giving the system a magnetically superelastic character. A further property of this alloy is that it also shows the inverse magnetocaloric effect. The magnetic superelasticity and the inverse magnetocaloric effect in Ni-Mn-In and their association with the first-order structural transition are studied by magnetization, strain, and neutron-diffraction studies under magnetic field.

DOI: 10.1103/PhysRevB.75.104414 PACS number(s): 75.80.+q, 61.12.−q

I. INTRODUCTION

Shape memory alloys exhibit unique thermomechanical properties which originate from a martensitic transition occurring between the austenite state with high crystallographic symmetry and a lower symmetry martensite state.[1] These materials are superelastic and can remember their original shape after severe deformation. Superelasticity is related to the stress-induced reversible structural transition.

Research on shape memory alloys received significant stimulus after the discovery of the magnetic shape memory (MSM) effect in Ni_2MnGa.[2] This effect arises from a magnetic-field-induced reorientation of twin-related martensitic variants and relies on high magnetocrystalline anisotropy. The driving force is provided by the difference between the Zeeman energies of neighboring martensite variants.[3,4] Giant strains up to 10% have been reported for off-stoichiometric Ni-Mn-Ga single variant crystals with the 14 M modulated martensitic structure.[5] Over the past decade, vast amount of knowledge accumulated on the properties of Ni-Mn-Ga Heusler alloys has enabled to foresee the possibility of employing these alloys in device applications.[6]

In applied magnetic fields, the martensitic start temperature M_s of Ni-Mn-Ga shifts to higher temperatures along with the other characteristic temperatures such as martensite finish M_f, austenite start A_s, and austenite finish A_f.[7] With this feature, it is possible to induce a reversible structural phase transformation, whereby strain can be fully recovered upon removal of the field without the necessity of prestraining the specimen.[8] In such magnetic-field-induced superelasticity, the maximum field-induced strain relies on the difference in the crystallographic dimensions in the martensitic and austenitic states. When a field of sufficient strength is applied at a temperature corresponding initially to the austenitic state, the shift in all characteristic temperatures (therefore the shift in the hysteresis associated with the transformation) can be large enough so that the martensitic state is stabilized. However, experiments performed in fields up to 10 T have shown that in the case of $Ni_{54}Mn_{21}Ga_{25}$ the rate of shift is only about $\sim 1\ KT^{-1}$.[8] Neutron-diffraction experiments under magnetic field on an alloy with similar composition confirm these results.[9]

Parallel to the development of the understanding of the MSM effect in Ni-Mn-Ga and exploiting giant strains for applications, the search for other MSM materials also took up considerable place in the research agenda.[10] In Ni-Co-Mn-In, it has recently been reported that when a magnetic field is applied to a prestrained single-crystal specimen, the strain is recovered with a value that is nearly equal to the size of the prestrain.[11] Although this is a considerable step in the search for magnetic superelasticity, a system in which considerable length change occurs reversibly by applying and removing a magnetic field without requiring prestrain is still to be found.

Recently, we have investigated a number of Ni-Mn based Heusler systems other than Ni-Mn-Ga with the aim of finding ferromagnetic alloys that undergo martensitic transformations and of understanding their properties around the transformation point.[12,13] In Ni-Mn-Sn,[14] we have come across an inverse magnetocaloric effect at temperatures in the range of the first-order martensitic transition with size comparable to that of the archetype $Gd_5(Si_{1-x}Ge_x)_4$ system, which exhibits the conventional giant magnetocaloric effect.[15]

Here, we demonstrate the presence of both magnetic superelasticity and the inverse magnetocaloric effect in Ni-Mn-In in the range of the martensitic transition. Large field-induced strains in polycrystalline Ni-Mn-In of magnitude similar to that in polycrystalline Ni-Mn-Ga are found. We show in Ni-Mn-In that instead of the large field-induced strain being due to twin boundary motion in the martensitic phase, it relies essentially on the reverse field-induced martensite-to-austenite transition. Below, we present results of field-dependent magnetization, calorimetry, neutron diffraction, strain, and length change measurements in magnetic field on a Ni-Mn-In alloy and discuss the field-induced strain

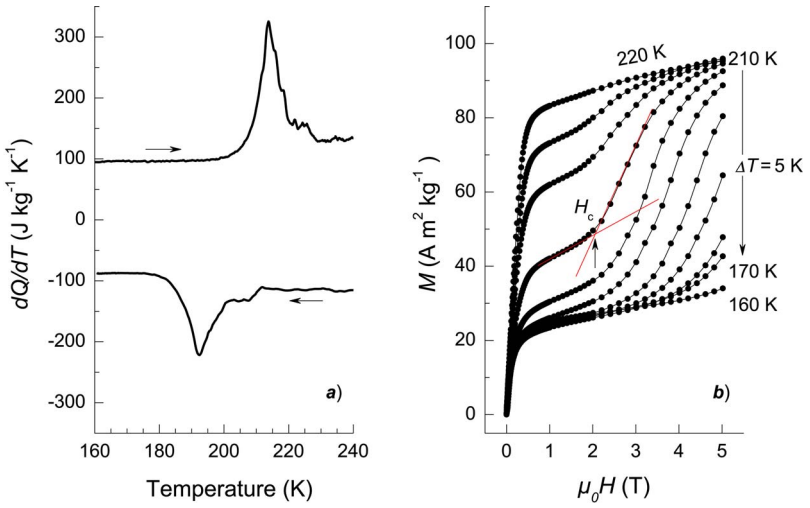

FIG. 1. (Color online) Features in the martensitic transformation associated with temperature and magnetic-field dependence. (a) Calorimetric curves across the martensitic transition. The horizontal arrows indicate the direction of temperature change. (b) Magnetization as a function of magnetic field measured on increasing field in the vicinity of the martensitic transition. The red (dark gray) lines drawn through the data points (shown only for the 200 K data) cross at a point corresponding to the characteristic field around which the metamagnetic transition begins to occur.

and the inverse magnetocaloric effect in relation to the field-induced martensite-to-austenite transition.

II. EXPERIMENT

Arc melted samples were annealed at 1073 K under argon atmosphere for 2 h and quenched in ice water. Magnetization measurements were carried out using a superconducting quantum interference device magnetometer, and calorimetric measurements in magnetic field were performed using a high-sensitivity differential scanning calorimeter.[16] Neutron diffraction in magnetic fields up to 5 T was performed on the D2B powder diffractometer at ILL, Grenoble. The strain measurements were made using conventional strain-gauge technique in magnetic fields up to 5 T.

III. RESULTS

A. Calorimetry and magnetization

$Ni_{50}Mn_{50-x}In_x$ alloys undergo martensitic transitions for about $x<16$.[17,13] Here we concentrate on the magnetostructural coupling in the ferromagnetic $Ni_{50.3}Mn_{33.8}In_{15.9}$ alloy, which has a Curie point $T_C=305$ K and transforms martensitically on cooling at $M_s=210$ K. The other characteristic temperatures defining the temperature limits of the transition are $M_f=175$ K, $A_s=200$ K, and $A_f=230$ K. These temperatures are determined from the calorimetry data in Fig. 1(a).

In order to search for the presence of a coupling of the structure with the magnetic degree of freedom within the temperature range of the martensitic transition, we have studied the field dependence of the magnetization $M(H)$. The data shown in Fig. 1(b) are obtained in increasing field and decreasing temperature. Here, the magnetizations in the temperature interval $160 \leqslant T \leqslant 210$ K initially show a tendency to saturate, but, then, exhibit metamagnetic transitions in higher fields. The characteristic field H_c defining the transition point is determined as the crossing point of the linear portions of the curves. The transition shifts to higher fields with decreasing temperature, and on removing the field, the magnetization returns to its original value (see Fig. 7). As will be shown with neutron diffraction in external field, the metamagnetic transition is associated with the onset of a field-induced reverse martensitic transition.

In Fig. 2, we show the relative length change $\Delta l/l$ as a function of temperature in different constant applied magnetic fields. As the field increases, M_s (indicated by arrows) decreases by an amount of about -10 KT^{-1}. The other characteristic temperatures are positioned in the conventional manner around the temperature hysteresis loop, and all shift by nearly the same amount in a given field. With increasing measuring field, the difference in $\Delta l/l$ between the austenitic and martensitic states decreases. The cause of this decrease is

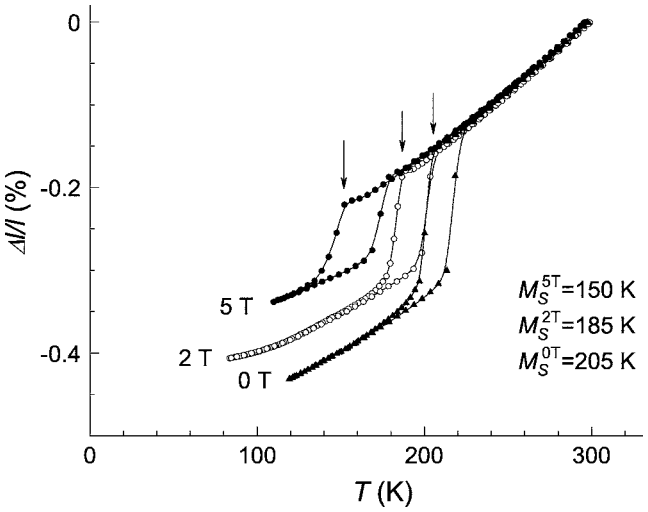

FIG. 2. The relative length change in constant applied magnetic fields of 0, 2, and 5 T. The arrows indicate the positions of M_s.

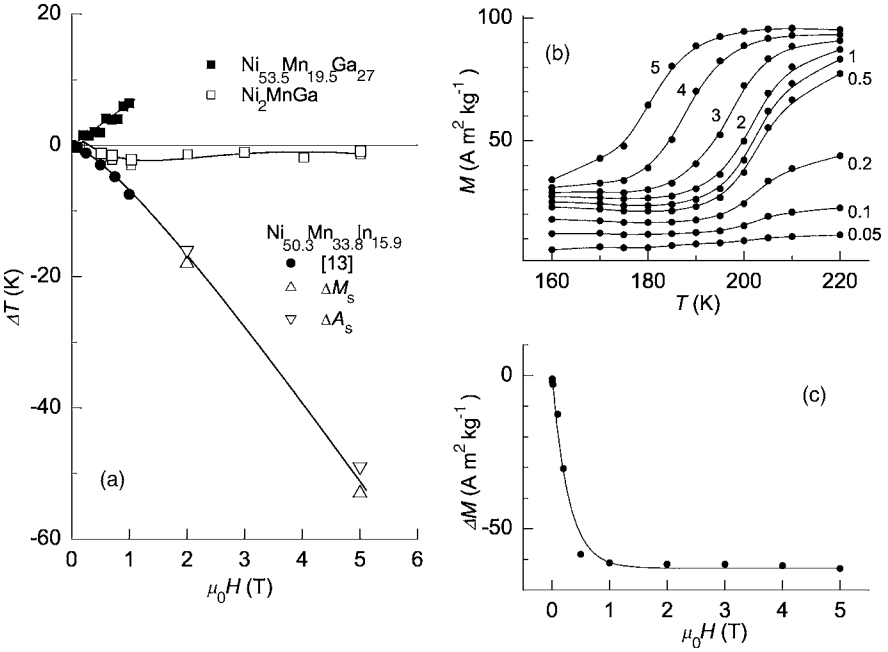

FIG. 3. Characteristic field-dependent properties around the martensitic transition. (a) Shift in the martensitic transition temperature as a function of magnetic field for $Ni_{50.3}Mn_{33.8}In_{15.9}$, Ni_2MnGa, and $Ni_{53.5}Mn_{19.5}Ga_{27}$. (b) Temperature dependence of the magnetization obtained at selected fields from Fig. 1(b). The numbers refer to magnetic field values in Tesla. (c) The difference between the magnetizations in the cubic and martensite phases. ΔM saturates at about 0.5 T. The lines drawn through the data are guides.

associated with the crystallographic orientation of the easy axis of magnetization within the orthorhombic structure of the martensitic phase. This property is discussed separately in Ref. 18.

In Fig. 3(a), we compare the magnitude of the shift of the transition temperatures represented by ΔT as a function of the external magnetic field $\mu_0 H$ of the present Ni-Mn-In alloy with those reported for Ni_2MnGa and $Ni_{53.5}Mn_{19.5}Ga_{27}$; the latter exhibiting the strongest field-dependent transition temperature.[19,20] Since the applied field shifts all characteristic temperatures by the same amount, ΔT is the change in any one of the characteristic transition temperatures in applied magnetic field with respect to zero field. The shifts in M_s and A_s of Ni-Mn-In determined from Fig. 2 are shown with up and down triangles, respectively. We have also included data for $\mu_0 H \leqslant 1$ T obtained from calorimetric measurements under constant magnetic field.[13]

Two significant features show up from Fig. 3(a): (i) the rate of change of the transition temperature in $Ni_{50.3}Mn_{33.8}In_{15.9}$ (-10 KT^{-1}) is higher than in $Ni_{53.5}Mn_{19.5}Ga_{27}$ (6 KT^{-1}), and (ii) in Ni-Mn-In, ΔT is negative, i.e., the transition temperature decreases with increasing field. This is consistent with the fact that the magnetization in the high-temperature cubic phase is larger than the magnetization in the martensitic phase as seen in Fig. 3(b), where the temperature dependence of the magnetizations at constant fields obtained from Fig. 1(b) at selected fields is plotted. The difference in the magnetization of the martensitic and austenitic states around the transition temperature ΔM is plotted as a function of applied field in Fig. 3(c).

B. Neutron diffraction in magnetic field

To understand the properties of the transition observed in $M(T)$ and $M(H)$, we have undertaken powder neutron-diffraction experiments as a function of temperature and magnetic field. The $Ni_{49.7}Mn_{34.3}In_{16.0}$ sample used for these experiments has a composition that differs slightly from that used in the measurements presented above and, therefore, the transition temperatures are slightly shifted. Therefore, we plot in Fig. 4 the $M(H)$ isotherms and compare these data to the neutron-diffraction data.

Figure 5(a) shows neutron-diffraction patterns at 5 and 317 K. The pattern at 317 K generates from an $L2_1$ structure

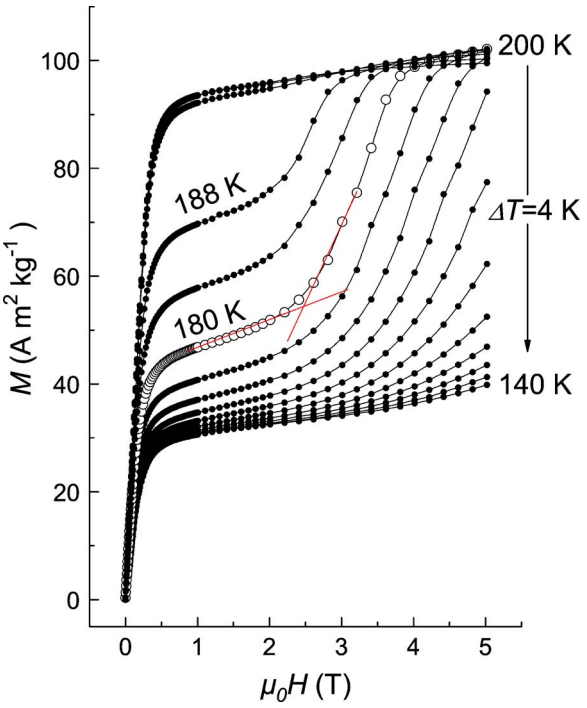

FIG. 4. (Color online) The magnetic-field dependence of the magnetization for the sample used in the neutron-diffraction experiments. The crossing point of the red (dark gray) lines determines H_c. The data with open symbols correspond to the isotherm at which the neutron-diffraction experiments were made.

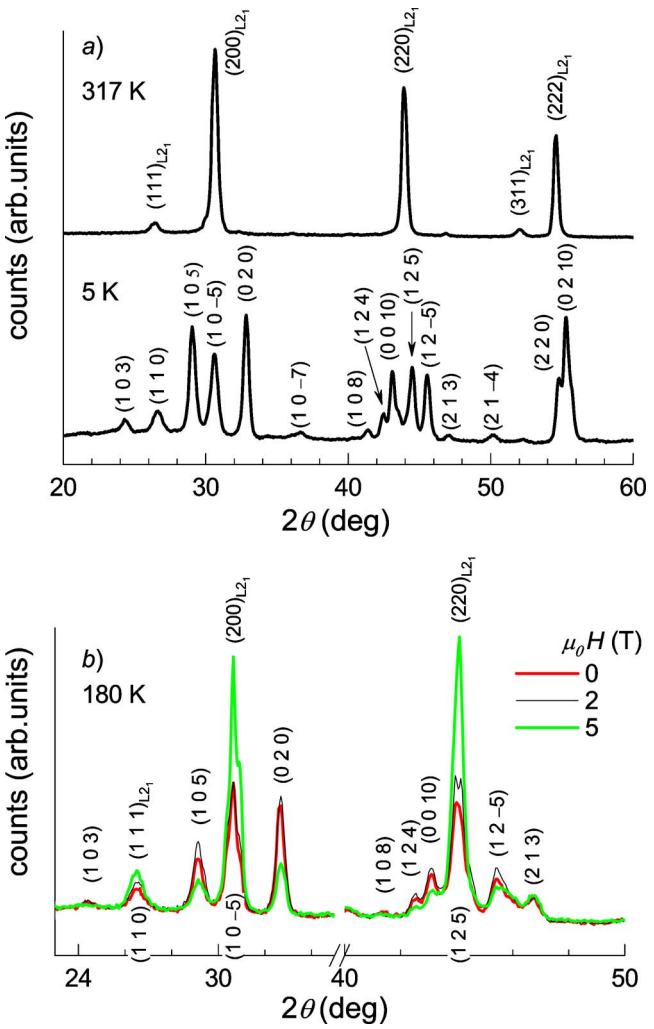

FIG. 5. (Color online) Neutron diffractograms. (a) Patterns at 317 K ($L2_1$) and 5 K (10 M martensite). (b) The field dependence of the diffraction pattern at 180 K showing the field-induced transformation from the martensite to the austenite state.

with a lattice constant $a=0.6011$ nm. At 5 K, the pattern is that of a 10 M modulated martensite structure having a monoclinic unit cell with $\beta=86.97°$ and lattice constants $a=0.4398$ nm, $b=0.5635$ nm, and $c=2.1720$ nm. Other than this slight monoclinicity, the structure is orthorhombic, having a shuffle periodicity of ten lattice planes in the [110] direction. In the pattern at 317 K, some additional weak reflections can be identified around 36° and 47°. These lie close to the positions of the (1 0 −7) and (2 1 3) reflections of the martensitic phase at 5 K, but at slightly smaller angles due to thermal expansion, and their presence is attributed to small amounts of mechanically induced martensite formed on grinding the ingot for powder specimen preparation.

At 180 K, which is a temperature that falls well in the range of the transformation (Fig. 4), we have studied the evolution of the diffraction spectrum with applied magnetic field. Figure 5(b) shows the spectrum in 2θ ranges that encompass the vicinity of the positions of the (200) and (220) reflections of the $L2_1$ phase. As the magnetic field increases, the intensities of these reflections grow at the expense of the

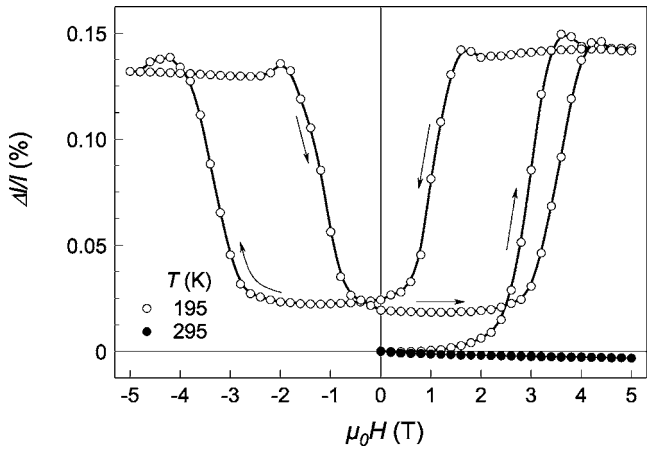

FIG. 6. Magnetic-field dependence of strain at 195 K ($T<M_s$) and 295 K ($L2_1$). The strain recovers on removing the field indicating magnetically superelastic behavior. Arrows show the direction of field change.

intensities of the (1 0 −5) and (1 2 5) reflections, which lie nearly at the same positions as the (200) and the (220) reflections of the $L2_1$ phase, respectively. This shows that a progressive magnetic-field-induced structural transition from the martensitic to the austenitic state is taking place with increasing magnetic field. In cases where the positions of the reflections pertain only to the martensitic phase, e.g., (1 0 5), (1 2 −5), etc., the intensity first increases with increasing magnetic field up to 2 T and, then, decreases. The initial increase is related to the increase in the magnetization in the martensitic state at 180 K up to around $\mu_0 H_c \approx 2$ T (Fig. 4). The subsequent decrease is associated with the gradual decrease in the amount of martensite and the stabilization of the $L2_1$ phase. However at 5 T, the reflections associated with the martensitic phase do not disappear, although their intensities are reduced. This indicates that the transition is not complete in this field, and larger magnetic fields are required to fully restore the $L2_1$ state at 180 K. The neutron-diffraction data indicate clearly a magnetic-field-induced reverse transition and give evidence that the observed metamagnetic transition in $M(H)$ is related to the reverse martensitic transition.

C. Magnetic-field-induced strain

The magnetic-field-induced structural phase transition in the present alloy can have important consequences on macroscopic strains occurring during the application of the field. Figure 6 shows the results of magnetic-field-dependent strain measurements, where the strain is defined as $\Delta l/l=[l(H)-l_0]/l_0$. Here, l_0 is the length in the absence of field and $l(H)$ the length in the presence of field. The sample is well within the austenitic temperature range at 295 K (filled circles) and is within the structural transition region at 195 K (open circles). The small field-induced strain at 295 K increasing negatively with increasing field corresponds to the intrinsic magnetostriction of the austenite, while at 195 K, a strain of about 0.14% is reached in the initial curve. After the first field cycle is completed, the strain reduces to about 0.12%

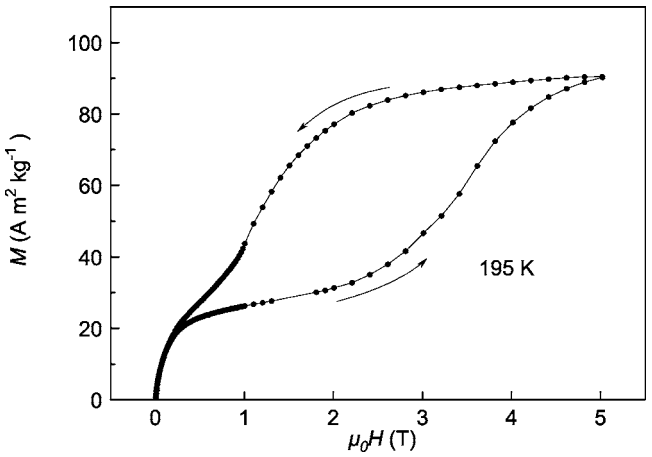

FIG. 7. The magnetic-field dependence of the magnetization at 195 K.

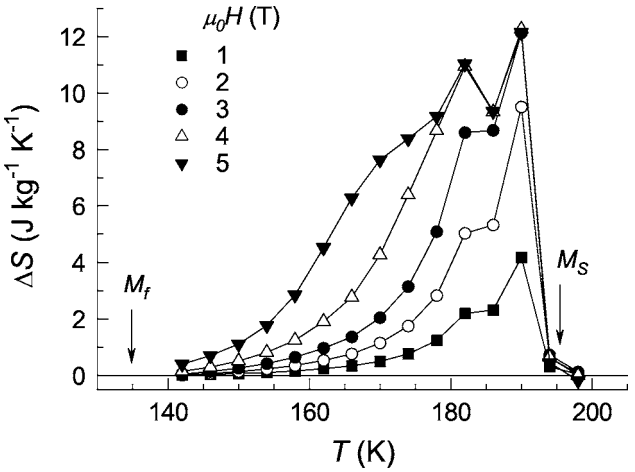

FIG. 8. Temperature dependence of ΔS.

and remains constant at this value, which is roughly the same as that attained in polycrystalline Ni-Mn-Ga. However, the effect here is due to the crystallographic transformation from martensite to austenite with increasing field-instead of a field induced twin boundary motion that occurs within the martensitic state as in Ni-Mn-Ga. Although hysteresis is observed in Fig. 6, the sample returns to its zero-field length upon removal of the field.

The features in the field dependence of the strain is reflected in the field dependence of the magnetization at the same temperature as seen in Fig. 7. The $M(H)$ curves show metamagnetic transitions around 2 and 1 T for the increasing and decreasing field branches, respectively. These points correspond to the fields where $\Delta l/l$ also changes rapidly. As in the case of $\Delta l/l$, $M(H)$ also shows essentially no remanence and recovers its zero-field value.

D. Magnetocaloric effect

Due to the first-order magnetic-field-induced transition and considerable difference in the magnetization of the martensitic and $L2_1$ states at the transition temperature, substantial magnetocaloric effects can be expected. The field-induced entropy change ΔS around the martensitic transition temperature can be estimated from magnetization measurements by employing the Maxwell equation[21]

$$\Delta S(T,H) = \mu_0 \int_0^H \left(\frac{\partial M}{\partial T}\right)_H dH, \tag{1}$$

from which the magnetocaloric effect can be evaluated by numerical integration using the data in Fig. 1(b). The resulting ΔS in the temperature range $170\ \mathrm{K} \leqslant T \leqslant 225\ \mathrm{K}$ is plotted in Fig. 8. The sign of ΔS is positive for all temperatures, indicating that an inverse magnetocaloric effect is present, i.e., the sample cools when a magnetic field is applied adiabatically as in Ni-Mn-Sn.[14] The maximum value of $\Delta S = 12\ \mathrm{J\ K^{-1}\ kg^{-1}}$ is reached in a magnetic field of 4 T at about 205 K. Since there is no substantial change in the magnetization above 4 T at this temperature, increasing the magnetic field any further does not lead to any further increase in ΔS. As expected for magnetostructural transitions,[22] this value is larger than the transition entropy change[13] since it also includes the effect of magnetization changes with temperature beyond the transition region.

IV. DISCUSSION

The origins of both distinct properties of the studied alloy, namely, the field-induced martensite-to-austenite transition and the inverse magnetocaloric effect, are related to the lower value of the magnetization in the martensitic phase with respect to that in the austenitic phase. The difference in the magnetization can be ascribed to the fact that in Mn-based Heusler alloys, the magnetic moments are localized mainly on the Mn atoms and the exchange interaction strongly depends on the Mn-Mn distance. Hence, any change in the distance caused by a change in the crystallographic configuration can modify the strength of the interactions, leading to different magnetic exchanges in each of the phases. Indeed, it has been shown in the case of a $Ni_{0.50}Mn_{0.36}Sn_{0.14}$ alloy that short-range antiferromagnetism is present between Mn atoms located at the 4(b) positions of the austenite phase, which is then strengthened in the martensitic state.[23] The present Ni-Mn-In alloy transforms to the same martensitic structure as in $Ni_{0.50}Mn_{0.36}Sn_{0.14}$. Therefore, the strong reduction of the magnetization below M_s in Ni-Mn-In can be expected to be due to a similar cause. The presence of short-range antiferromagnetism in the ferromagnetic matrix leads to frustration in the temperature range of the martensitic transition. In such a frustrated system, the application of a magnetic field can lead to the degeneracy of the spin states, giving rise to an increase in the configurational entropy that is required for the observed positive ΔS. However, the quantitative details of the frustrated state and the microscopic process leading to a positive ΔS remain to be described.

In Ni-Mn-Ga, giant strains are due to the reorientation of twin-related variants in the martensitic state, and recovery of this strain is, in general, not achieved by simply removing the field. By contrast, the magnetic superelastic effect and the associated strain reported here for Ni-Mn-In are related

to the field-induced structural transition. This enables one to reversibly induce and recover the strain by simply applying and removing the field.

V. CONCLUSION

$Ni_{0.50}Mn_{0.34}In_{0.16}$ exhibits a magnetic-field-induced structural transition from the martensitic state to the austenitic state. The transition is directly evidenced by neutron-diffraction measurements under magnetic field. Here, other than in Ni-Mn-Ga alloys, where the magnetization of the martensitic state is higher than that in the cubic phase, the austenite is stabilized by the application of a magnetic field. The shift of the transition temperatures was found to be large and negative with values up to about −50 K in 5 T. Due to the reversible magnetic-field-induced transition, magnetic superelasticity with 0.12% strains occur. Other than in magnetic shape memory alloys, where strain is mainly created by twin boundary motion, strain in $Ni_{0.50}Mn_{0.34}In_{0.16}$ is caused by changes in lattice parameters during the transition. Additionally, an inverse magnetocaloric effect with a maximum value in the entropy change of about 12 J kg^{-1} K^{-1} at 190 K and a minimum entropy change of 8 J kg^{-1} K^{-1} in a broad temperature range 170 K $\leqslant T \leqslant$ 190 K is also found in this alloy.

ACKNOWLEDGMENTS

We thank Peter Hinkel and Sabine Schremmer for technical support. This work was supported by Deutsche Forschungsgemeinschaft (GK277) and CICyT (Spain), Project No. MAT2004-1291. X.M. acknowledges support from DGICyT (Spain).

[1] *Shape Memory Materials*, edited by K. Otsuka and C. M. Wayman (Cambridge University Press, Cambridge, 1998).
[2] K. Ullakko, J. K. Huang, C. Kantner, R. C. O'Handley, and V. V. Kokorin, Appl. Phys. Lett. **69**, 1966 (1996).
[3] R. C. O'Handley, J. Appl. Phys. **83**, 3263 (1998).
[4] R. D. James and M. Wuttig, Philos. Mag. A **77**, 1273 (1998).
[5] A. Sozinov, A. A. Likhachev, N. Lanska, and K. Ullakko, Appl. Phys. Lett. **80**, 1746 (2002).
[6] K. Kakeshita and K. Ullakko, MRS Bull. **27**, 105 (2002).
[7] A. D. Bozhko, A. N. Vasil'ev, V. V. Khovailo, I. E. Dikshtein, V. V. Koledov, S. M. Seletskii, A. A. Tulaikova, A. A. Cherechukin, and V. D. Buchel'nikov, JETP **88**, 954 (1999).
[8] I. E. Dikshtein, D. I. Ermakov, V. V. Koledov, L. V. Koledov, T. Tagaki, A. A. Tulaikova, A. A. Cherechukin, and V. G. Shavrov, JETP Lett. **72**, 373 (2000).
[9] K. Inoue, K. Enami, Y. Yamaguchi, K. Ohoyama, Y. Morii, Y. Matsuoka, and K. Inoue, J. Phys. Soc. Jpn. **69**, 3485 (2000).
[10] M. Wuttig, L. Liu, K. Tsuchiya, and R. D. James, J. Appl. Phys. **87**, 4707 (2000).
[11] R. Kainuma, Y. Imano, W. Ito, Y. Imano, W. Ito, Y. Sutou, H. Morito, S. Okamoto, O. Kitakami, K. Oikawa, A. Fujita, T. Kanomata, and K. Ishida, Nature (London) **439**, 957 (2006).
[12] T. Krenke, M. Acet, E. F. Wassermann, X. Moya, L. Mañosa, and A. Planes, Phys. Rev. B **72**, 014412 (2005).
[13] T. Krenke, M. Acet, E. F. Wassermann, X. Moya, L. Mañosa, and A. Planes, Phys. Rev. B **73**, 174413 (2006).
[14] T. Krenke, M. Acet, E. F. Wassermann, X. Moya, L. Mañosa, and A. Planes, Nat. Mater. **4**, 450 (2005).
[15] V. K. Pecharsky and K. A. Gschneidner, Jr., Phys. Rev. Lett. **78**, 4494 (1997).
[16] J. Marcos, F. Casanova, X. Batlle, A. Labarta, A. Planes, and L. Mañosa, Rev. Sci. Instrum. **74**, 4768 (2003).
[17] Y. Sutou, Y. Imano, N. Koeda, T. Omori, R. Kainuma, K. Ishida, and K. Oikawa, Appl. Phys. Lett. **85**, 4358 (2004).
[18] T. Krenke and M. Acet (unpublished).
[19] J. Kim, F. Inaba, T. Fukuda, and T. Kakeshita, Acta Mater. **54**, 493 (2006).
[20] S. Jeong, K. Inoue, S. Inoue, K. Koterazawa, M. Taya, and K. Inoue, Mater. Sci. Eng., A **359**, 253 (2003).
[21] O. Tegus, E. Brück, L. Zhang, Dagula, K. H. J. Buschow, and F. R. de Boer, Physica B **319**, 174 (2002).
[22] F. Casanova, X. Batlle, A. Labarta, J. Marcos, L. Mañosa, and A. Planes, Phys. Rev. B **66**, 100401(R) (2002).
[23] P. J. Brown, A. P. Gandy, K. Ishida, R. Kainuma, T. Kanomata, K. U. Neumann, K. Oikawa, B. Ouladdiaf, and K. R. A. Ziebeck, J. Phys.: Condens. Matter **18**, 2249 (2006).